NIH Public Access
Author Manuscript
Cancer Res. Author manuscript; available in PMC 2014 February 01.

Published in final edited form as:
Cancer Res. 2013 February 1; 73(3): 1201–1210. doi:10.1158/0008-5472.CAN-12-2989.

CCR2 deficiency prevents neuronal dysfunction and cognitive impairments induced by cranial irradiation

Karim Belarbi[1,2], **Timothy Jopson**[1,2], **Carla Arellano**[1,2], **John R. Fike**[1,3], and **Susanna Rosi**[1,2,3]

[1]Brain and Spinal Injury Center, University of California, San Francisco, CA, USA

[2]Department of Physical Therapy Rehabilitation Science, University of California, San Francisco, CA, USA

[3]Department of Neurological Surgery, University of California, San Francisco, CA, USA

Abstract

Cranial irradiation can lead to long-lasting cognitive impairments in patients receiving radiotherapy for the treatment of malignant brain tumors. Recent studies have suggested inflammation as a major contributor to these deficits; we determined if the chemokine receptor 2 (CCR2) was a mediator of cognitive impairments induced by irradiation. Two-month-old male Ccr2 knockout (−/−) and wild-type (WT) mice received 10 Gy cranial irradiation or sham-treatment. One month after irradiation, bromodeoxyuridine was injected intraperitoneally for seven consecutive days to label newly generated cells. At two months post-irradiation, cognitive function was assessed by novel object recognition and Morris water maze. Our results demonstrate that CCR2 deficiency prevented hippocampus-dependent spatial learning and memory impairments induced by cranial irradiation. Hippocampal gene expression analysis showed that irradiation induced CCR2 ligands such as CCL8, and CCR2 deficiency reduced this induction. Irradiation reduced the number of adult-born neurons in both WT and Ccr2−/− mice, but the distribution pattern of the adult-born neurons through the granule cell layer was only altered in WT mice. Importantly, CCR2 deficiency normalized the fraction of pyramidal neurons expressing the plasticity-related immediate early gene Arc. These data offer new insight into the mechanism(s) of radiation-injury and suggest that CCR2 is a critical mediator hippocampal neuronal dysfunction and hippocampal cognitive impairments after irradiation. Targeting CCR2 signaling could conceivably provide an effective approach to reduce or prevent the incidence and severity of this serious side effect of ionizing irradiation.

Keywords

adult neurogenesis; chemokine; cognition; hippocampus; irradiation

Introduction

Ionizing radiation is a frontline treatment for intracranial malignancies. However, cranial irradiation can induce a progressive and long-lasting decline in cognition that can severely impact the quality of life (1, 2). Such deficits can manifest in humans and experimental models as hippocampus-dependent impairments that involve spatial information processing (3, 4). It has been suggested that the severity of cognitive impairment in humans depends upon the dose

Corresponding author: Susanna Rosi, PhD, Brain and Spinal Injury Center, University of California San Francisco, San Francisco General Hospital, 1001 Potrero Ave, Bld#1, Room#101 94110, San Francisco, CA. Office: 415 206 3708, Lab: 415 206 8747, Fax: 415 206 3948, rosis@ptrehab.ucsf.edu.

Competing interests: the authors declare that they have no competing interests.

NIH-PA Author Manuscript
NIH-PA Author Manuscript
NIH-PA Author Manuscript

NIH-PA Author Manuscript

NIH-PA Author Manuscript

NIH-PA Author Manuscript

of radiation delivered to the medial temporal lobes (1), where the hippocampus is located. Given the growing population of long-term survivors of intracranial tumor, quality of life has become an increasing concern (2). Currently, there are no successful treatments or prevention strategies for radiation-induced cognitive impairments, and only a few possibilities have been suggested (5, 6). Therefore there is a need to more fully understand the pathogenesis of cognitive dysfunctions after irradiation so that new approaches or strategies to treat this serious complication can be developed.

While high radiation doses can lead to serious damage involving tissue destruction (7), the mechanisms underlying lower dose radiation-induced cognitive impairments are likely to be subtle and multifactorial. Important possibilities include alterations in the neurogenic cell populations in the dentate gyrus (DG) (3, 8, 9) as well as changes in functional activation of neuronal networks of the hippocampus (10). New neurons (adult-born) are generated in the subgranular zone of the DG (11) and migrate into the granule cell layer, where they integrate into hippocampal networks (12–14) and contribute to hippocampal function (15, 16). We and others have demonstrated that ionizing irradiation reduces the production of adult-born neurons (3, 8, 12, 17), alters the distribution of remaining adult-born neurons throughout the granule cell layer (12), and disrupts the activity patterns associated with neuroplasticity in hippocampal neurons (10). Importantly, several studies suggest that inflammatory factors may adversely affect adult neurogenesis (13, 18, 19), contribute to the disruption of neuronal function, and negatively impact accuracy of hippocampal network activity (20–22) and cognitive function (23). Taken together, data from a number of laboratories suggest that inflammation may play a causal if not contributory role in the pathogenesis of radiation induced cognitive deficits.

Due to their ability to regulate immune cell activation (24), chemokine receptors and their ligands are considered essential mediators of post-injury neuroinflammation. Cells of the monocyte-macrophage lineage, including microglia, express the chemokine (C-C motif) receptor (CCR) 2 (25–27) and studies using CCR2 knockout mice have shown its crucial and non-redundant role in peripheral macrophage infiltration at the sites of injury in the central nervous system (CNS) (28–30). Moreover, CCR2 is also expressed by neural progenitors (31) and by mature granular and pyramidal neurons of the hippocampus (32, 33) and could therefore modulate both neurogenesis and neuronal function in the hippocampus. Additionally, CCR2 has been shown to play a role in the pathogenic processes in several models of neurological disorders (29, 34, 35). Given those data, it is conceivable that after brain irradiation CCR2 signaling may have an important influence on inflammation, neurogenesis, hippocampal neuronal activity and cognitive functions. To test this hypothesis we used our well established mouse model of cranial irradiation (3, 8, 10, 36) and measured cognitive functions, expression of inflammatory cytokines and their receptors, macrophage/microglia activation, adult neurogenesis and hippocampal neuronal network activation, in wild-type (WT) mice, and mice lacking CCR2 ($CCR2^{-/-}$).

Materials and Methods

Animal procedures

This research was conducted in compliance with the United States Department of Health and Human Services Guide for the Care and Use of Laboratory Animals and with the University of California Institutional Animal Care and Use Committee. Two-month-old $CCR2^{-/-}$ mice on a C57BL/6 background and WT C57BL/6 mice were purchased from The Jackson Laboratory (Bar Harbor, ME). All animals were anesthetized with an intraperitoneal (i.p) injection of a ketamine (100mg/kg)/xylazine (10mg/kg) mixture, placed 16.3 cm from a cesium-137 source (J.L. Shepherd & Associates). The body was shielded with a lead collimator that limited the beam to a width of 1 centimeter. Irradiated animals ($CCR2^{-/-}$-IRR n=10 and WT-IRR n=10) were given a single 10 Gy dose to the head only. Sham animals ($CCR2^{-/-}$-SH

NIH-PA Author Manuscript

NIH-PA Author Manuscript

NIH-PA Author Manuscript

n=10 and WT-SH n=10) were treated identically without being exposed to irradiation. Four weeks post-irradiation, mice were injected with bromodeoxyuridine (BrdU; Sigma-Aldrich; 100mg/kg/day; i.p.; 7 days) to label cells synthesizing DNA. Mice were handled daily for 10 days prior to behavioral assessment. Behavioral manipulations and testing were carried out during reversed light cycle. Novel object recognition training and testing was conducted 10 weeks post-irradiation and lasted 5 days, as described below. Morris water maze test began at 11 weeks post-irradiation and lasted 5 days (see details below). Each mouse was euthanized 25 min after completion of the last trial of the Morris water maze (82 days post-irradiation), and the brain was quickly removed and divided at the midline as previously described (10). One hemisphere was immediately frozen in −70 °C isopentane (Sigma-Aldrich) for histological analysis and the hippocampus of the other hemisphere was removed at 4°C and stored at −70° C for further RNA extraction.

Novel object recognition

Hippocampus-independent functions (37) were measured using the novel object recognition test. Briefly, an open field arena (60×60 cm square with 20 cm high walls) was placed in a dimly lit behavioral testing room. Large visual cues were placed on the walls of the testing room at various locations to provide spatial points of reference. Mice were allowed to explore the open field arena for one 5-minute period for 4 consecutive days (habituation phase). On Day 5, three identical objects were placed in the arena and mice were allowed to explore them for four 10-minute periods (familiarization phase). Mice were then placed back in their cage for 4 minutes. One of the objects was then replaced with a novel object and mice were reintroduced into the open arena to explore for 3 minutes. Trials were recorded using an overhead camera and live tracking of the animals was achieved using an automated video tracking system (Ethovision XT; Noldus Information Technology). Exploratory behavior was defined as the animal directing its nose toward an object at a distance of < 4cm. Data were expressed as the percent time spent exploring the novel object relative to the total time spent exploring all the objects. The objects were secured to the floor using Velcro. The arena and objects were cleaned with 0.025% bleach between trials to minimize odor cues.

Morris water maze

Assessment of hippocampus-dependent cognitive performance was performed using the Morris water maze test (38). A plastic tank/pool (120 cm diameter) was placed in a dimly lit behavioral testing room. Visual cues were placed around the room as spatial references. A transparent platform (10 cm diameter) was placed in the tank and opaque water was added until the platform was submerged 1 cm below the surface. Visible platform training took place on Day 1, with a flag installed on the escape platform to allow the mouse to see the location of the platform. Each mouse performed a total of 6 visible platform trials, with the platform placed at different locations in each trial. A mouse that failed to locate the platform within the allotted time was immediately guided to the platform manually. Once the mouse reached the platform, it remained there for 20 seconds before removal from the water maze. Hidden platform training took place on Days 2–4. All mice performed 6 trials per day (18 trials total), and the tank insertion point was changed randomly from trial to trial. The maximum trial duration was 60 seconds, after which animals were manually guided to the platform in the event that they failed to locate it and were allowed to remain there for 20 seconds. On Day 5, the platform was removed and animals were allowed to swim freely for 60 seconds. Memory consolidation (to test if the animals remembered what they learned the previous day) was measured with the first trial of each day (24 hours after the last trial performed on the previous day). Ethovision automated video tracking system (Noldus Information Technology) monitored all performances in the following parameters: average velocity and distance to platform zone.

NIH-PA Author Manuscript

NIH-PA Author Manuscript

NIH-PA Author Manuscript

RNA extraction and transcript analyses

The hippocampus from each mouse was processed for total RNA extraction and purification using the RNeasy Lipid Tissue Mini Kit (Qiagen). For PCR array-based gene expression analysis, RNAs from mice in the same experimental group were initially pooled to yield one RNA sample per group. One microgram total RNA from each pooled sample was reverse-transcribed into cDNA using the RT^2 First Strand Kit (SABiosciences, Qiagen) according to the protocol provided by the manufacturer. Gene expression analysis was performed on a Mx3005P QPCR System (Agilent Technologies) using Mouse Inflammatory Cytokines & Receptors RT^2 Profiler PCR Array (SABiosciences, Qiagen) according to the manufacturer's specification. Gene expression was calculated using the PCR Array Data Analysis template (SABiosciences, Qiagen). For analyzing expression levels of one individual target genes on a per animal basis, one microgram of total RNA from each mouse was reverse-transcribed using the High-Capacity cDNA reverse transcription kit (Applied Biosystems). Quantitative real-time RT-PCR analysis was performed on Mx3005P QPCR System (Agilent Technologies) using Brilliant II SYBR Green reagents (Stratagene). The thermal cycler conditions were as follows: hold for 10 min at 95°C, followed by 40 cycles of a two-step PCR consisting of a 95° C step for 30 s followed by a 60°C step for 1 min. Primer sequences are presented in table 1. Amplifications were carried out in triplicate and the relative expression of target genes was determined by the ΔΔCT method using cyclophilin gene expression as an internal control to normalize the results.

Histological procedures

Brain tissue was blocked as previously described (12) such that each block contained a hemisphere from one mouse from each experimental group. These blocks were then cryosectioned at a thickness of 20 μm and the coronal brain slices collected on microscopic slides. All slides were stored at −70 °C until processed for immunohistochemistry. Sections were selected from the medial portion of the dorsal hippocampus (from 3.2 to 4.00 mm posterior to bregma) and stained for: 1) mature neurons (NeuN monoclonal antibody clone A60; Chemicon), 2) BrdU (BrdU mouse monoclonal antibody clone BMC9318; Roche Applied Science) and 3) Arc protein (Arc rabbit polyclonal antibody; Synaptic Systems). Specific technical details, including antibody and other reagent concentrations, have been recently reported by us (13, 14, 20).

Image acquisition and analysis

Z-stack images (200X magnification; 1 μm optical thickness per plane; 8 planes) of the DG the CA1 and the CA3 areas were taken using a Zeiss Apotome microscope; offline analyses were performed using Zeiss AxioVision software. The percentage of Arc immunoreactive neurons from the entire DG enclosed blade and the CA1 and CA3 areas (two counting frames/area/slide) were assessed using two stained slides from the dorsal hippocampus as described in detail previously (12, 13). The distribution of adult-born neurons throughout the enclosed blade of the dentate granule cell layer was analyzed as follows: for each BrdU-labeled neuron, the distance between the center of the nucleus and the subgranular zone (distance of migration = m) and the width of the granule cell layer (width = w) were measured. This value was defined as index of migration was calculated as $i_m = m/w \times 100$ (13).

Statistics

Results were expressed as fold changes ± SEM (Array data) or means ± SEM (behavior, real-time RT-PCR, histology data). Differences between mean values were determined using t-test or one-way analysis of variance (ANOVA) procedures with Newman-Keuls tests for post hoc comparison. The learning curve of the Morris water maze hidden platform training was analyzed with a two-way ANOVA with day and experimental group as independent factors

NIH-PA Author Manuscript

NIH-PA Author Manuscript

NIH-PA Author Manuscript

and with Bonferroni tests for post hoc comparisons. Values of $p \leq 0.05$ were considered to be statistically significant. Data were analyzed and graphs were plotted by GraphPad Prism software version 5.0c.

Results

In accordance with previous studies (10, 36), whole-brain irradiation with 10 Gy as used here was tolerated by all animals. All mice gained weight normally over the duration of the study (not shown).

Irradiation did not impact novel object recognition

Analysis of the total time spent exploring the objects during the familiarization phase revealed no significant difference between groups (F=0.7497; p=0.053; Fig. 1a). During the test phase, animals from all experimental groups showed a significant discrimination between the novel and familiar objects, spending significantly more time exploring the novel object (WT-SH: F=38.89, p<0.0001; WT-IRR: F=110.4, p<0.0001; CCR2$^{-/-}$-SH: F=30.09, p<0.0001; CCR2$^{-/-}$-IRR: F=17.72, p<0.0001; Fig. 1b). Thus, neither irradiation nor CCR2 deficiency altered hippocampus-independent novel object recognition.

Irradiation impaired spatial learning and memory in WT but not in CCR2$^{-/-}$ mice

During the visible platform training in the Morris water maze, there was no significant group difference in average swim velocity (F=0.4448; p=0.7225; Fig. 2a) or swim path to the platform (F=0.8146; p=0.4948; Fig. 2b *left*, day 1, visible platform). This demonstrated that neither irradiation nor CCR2 deficiency induced any impairment in motor function or visual acuity. Repeated measures ANOVA of the distance path to the hidden platform, for each daily session, revealed significant differences between groups (F=3.013; p=0.0439) and across sessions (F=74.36; *P*<0.0001) with no significant interaction (*F*=1.643; p=0.1494). Repeated measures ANOVA for each group showed that WT-SH (F=11.76; p=0.0010), WT-IRR (F=18.56; p<0.0001), CCR2$^{-/-}$-SH (F=22.21; p<0.0001) and CCR2$^{-/-}$-IRR (F=30.78; p<0.0001) groups had a significant difference across sessions, indicating that all groups showed daily improvements in their abilities to locate the hidden platform (Fig. 2b). However, both WT-IRR (p<0.01) and CCR2$^{-/-}$-SH (p<0.001) mice showed significantly longer swim path to the platform than the WT-SH on day 2 (hidden platform training; Fig. 2b). Furthermore, irradiation induced spatial memory deficits in WT mice as revealed by the significantly longer swim path to the platform zone of the WT-IRR group on the first trial of day 3 and 4 (24 hs memory test) compared with the other groups (Day 3 overall ANOVA, F=3.305; p=0.0321; WT-IRR vs. WT-SH, p<0.05, WT-IRR vs. CCR2$^{-/-}$-SH, p<0.05 and WT-IRR vs. CCR2$^{-/-}$-IRR, p<0.05; Day 4 overall ANOVA, F=3.996; p=0.0156; WT-IRR vs. WT-SH, p<0.05, WT-IRR vs. CCR2$^{-/-}$-SH, p<0.05 and WT-IRR vs. CCR2$^{-/-}$-IRR, p<0.05; Fig. 2c). The CCR2$^{-/-}$-IRR group was not statistically different from the WT-SH or CCR2$^{-/-}$-SH groups. Together, these findings show that irradiation impaired spatial memory acquisition and consolidation in WT mice, and that CCR2 deficiency prevented this radiation induced deficit.

Irradiation-induced expressions of CCL8 and CCR1 were downregulated by CCR2 deficiency

As a first attempt to identify specific factors that regulated inflammation and whose expression was impacted by irradiation and/or CCR2 deficiency, we pooled samples from the various experimental groups and performed a PCR-based array to screen changes in levels of cytokines and receptors. Among the 84 factors examined, significant increases in CCL7, CCL8, CCL12 and CCR1 mRNAs were seen in the WT-IRR mice compared with WT-SH mice (11.10, 2.89, 3.06 and 9.21 fold-changes, respectively; Table 2). Comparison of gene expression in CCR2$^{-/-}$-SH compared with WT-SH showed that CCR2 deficiency was paralleled by a decreased expression of other chemokine receptors such as CCR3, CCR5 and CCR9 (−5.47,

NIH-PA Author Manuscript

NIH-PA Author Manuscript

NIH-PA Author Manuscript

−3.79 and −3.73 fold-changes, respectively). Although the cytokines CCL7, CCL8, CCL12 and receptors CCR1 were upregulated in $CCR2^{-/-}$-IRR mice (2.96, 2.41, 3.79 and 4.53 fold-changes, respectively), their inflammatory profile differed significantly from that of WT-IRR mice. Of particular interest, the large elevation of CCL8, known to be a ligand for CCR2, appeared drastically downregulated in $CCR2^{-/-}$-IRR deficient mice when compared with WT-IRR controls (−4.51 fold-change; Table 2). To analyze the changes in expression of factors identified in the screening, quantitative real-time RT-PCR analyses were performed on a per animal basis. Obtained data demonstrate that irradiation induced a statistically significant increase in the gene expression of the chemokines CCL7 ($F=7.027$ $p=0.0009$; post hoc tests: WT-IRR vs. WT-SH, $p<0.05$, $CCR2^{-/-}$-IRR vs. $CCR2^{-/-}$-SH, $p<0.01$) CCL8 ($F=10.35$ $p<0.001$; post hoc tests: WT-IRR vs. WT-SH, $p<0.001$, $CCR2^{-/-}$-IRR vs. $CCR2^{-/-}$-SH, ns) CCL12 ($F= 17.36$ $p<0.0001$; post hoc tests: WT-IRR vs. WT-SH, $p<0.001$, $CCR2^{-/-}$-IRR vs. $CCR2^{-/-}$-SH, $p<0.001$) and CXCL4 ($F=7.358$ $p=0.0006$; post hoc tests: WT-IRR vs. WT-SH, $p<0.001$, $CCR2^{-/-}$-IRR vs. $CCR2^{-/-}$-SH, $p<0.001$) and of the chemokine receptors CCR1 ($F= 44.72$ $p<0.0001$; post hoc tests: WT-IRR vs. WT-SH, $p<0.001$, $CCR2^{-/-}$-IRR vs. $CCR2^{-/-}$-SH, $p<0.01$) and CCR2 ($F=18.69$; post hoc tests: WT-IRR vs. WT-SH, $p<0.01$) (Fig. 3a and b). Importantly, statistically significant differences between WT-IRR mice and $CCR2^{-/-}$-IRR mice were observed for CCR1 ($p<0.001$) and CCL8 ($p<0.001$). Our data therefore show that irradiation induces expression of the ligands CCL7, CCL8, CCL12 and CXCL4 and of the receptor CCR1, CCR2 and that CCR2 deficiency affects this response, most notably with respect to CCL8 and CCR1.

Irradiation upregulated M2 macrophage markers in WT and $CCR2^{-/-}$ mice

Quantitative RT-PCR analyses of hippocampus tissues were used to assess molecular markers related to macrophage activation. Expression of the pan-macrophage marker CD68 did not differ significantly between groups ($F=1.126$; $p=0.35$; Fig. 3c). To further characterize macrophage activation, we separated the classical (pro-inflammatory) and alternative (anti-inflammatory) phenotypes of macrophages/microglia (also called M1 and M2 phenotypes, respectively) using specific molecular markers (39, 40). No significant changes in the M1 phenotype markers iNOS or CD16 were observed between experimental groups ($F=0.2728$; $p=0.8445$ and $F=2.425$; $p=0.0826$, respectively; Fig. 3c). In contrast, the M2 phenotype marker CD206 was significantly increased in WT-IRR mice compared with WT-SH mice ($F=4.272$; $p=0.0116$; WT-IRR vs. WT-SH, $p<0.05$; Fig. 3c). Although the CD206 elevation was not as great in $CCR2^{-/-}$ mice, the same trend was observed. Likewise, the M2 marker Ym1 was elevated in both WT-IRR and $CCR2^{-/-}$-IRR mice compared with their respective non-irradiated controls, although it did not reach statistical significance in either group (Fig. 3c). No significant changes in arginase were observed between experimental groups. In conclusion, irradiation tended to increase several M2 but not M1 markers in both WT and CCR2 deficient mice.

Irradiation reduced the number of adult-born neurons in both WT and $CCR2^{-/-}$ mice

NeuN immunostaining showed no gross changes between experimental groups in neither hippocampal morphology nor significant hippocampal neuronal loss (data not shown), in line with previous studies (10). Analysis of the number of BrdU-labeled neurons (BrdU+/NeuN+) revealed significant differences between groups ($F=62.12$, $p<0.0001$) with lower values observed in irradiated animals than in non-irradiated controls (WT-IRR vs. WT-SH, $p<0.001$, WT-IRR vs $CCR2^{-/-}$-SH $p<0.001$, $CCR2^{-/-}$-IRR vs. WT-SH, $p<0.001$ and $CCR2^{-/-}$-IRR vs. $CCR2^{-/-}$-SH, $p<0.001$). The WT-IRR group was not statistically different from the $CCR2^{-/-}$-IRR group (Fig. 4a). Therefore, while irradiation decreased the number of adult-born neurons, this effect was independent of CCR2 genotype.

NIH-PA Author Manuscript

NIH-PA Author Manuscript

NIH-PA Author Manuscript

Irradiation altered the distribution of adult-born neurons in WT but not in CCR2$^{-/-}$ mice

Distribution analysis of adult born neurons (Fig. 4b and c) revealed that the average index of migration of BrdU-labeled neurons was higher in WT-IRR mice than in WT-SH, CCR2$^{-/-}$-SH and CCR2$^{-/-}$-IRR mice (overall ANOVA, F=8.100; p<0.0001; post hoc tests: WT-IRR vs. WT-SH, p<0.001, WT-IRR vs. CCR2$^{-/-}$-SH, p<0.001 and WT-IRR vs. CCR2$^{-/-}$-IRR, p<0.01). The proportions of BrdU-labeled neurons found in the inner, mid and the outer third of the enclosed blade of the DG were compared between the different experimental groups using one-way ANOVA (Fig. 4d). The proportion of cells in the inner third layer differed statistically between groups (F=5.468; p=0.0033), where the proportion of BrdU-positive cells found in WT-IRR mice was significantly lower from all other groups (post hoc tests: WT-IRR vs. WT-SH, p<0.01, WT-IRR vs. CCR2$^{-/-}$-SH, p<0.01 and WT-IRR vs. CCR2$^{-/-}$-IRR, p<0.01). The proportion of BrdU-positive neurons in the mid-third layer did not differ significantly among groups (F=0.6167; p=0.6087). In the outer third layer, significant differences were found in the proportion of BrdU-positive neurons among groups (F=6.034; p=0.0019) and post hoc analysis revealed differences between WT-IRR mice and all other groups (WT-IRR vs. WT-SH, p<0.01, WT-IRR vs CCR2$^{-/-}$-SH, p<0.01 and WT-IRR vs CCR2$^{-/-}$-IRR, p<0.01). DG enclosed blade width was comparable between WT-SH, WT-IRR, CCR2$^{-/-}$-SH and CCR2$^{-/-}$-IRR mice (data not shown). In conclusion, the higher average index of migration in WT-IRR mice and the differences in the proportion of cells located in the different regions indicated that irradiation altered the distribution of remaining adult-born neurons throughout the granule cell layer in WT-IRR mice but not in CCR2$^{-/-}$-IRR mice.

Irradiation altered the expression of behaviorally-induced Arc protein in the hippocampus in WT but not in CCR2$^{-/-}$ mice

To establish how irradiation affected spatial information processing and the impact of CCR2 deficiency from a cellular and network prospective, after the last trial of the Morris water maze we analyzed the proportion of neurons expressing the plasticity-related immediate early gene Arc in the DG, CA1 and CA3 areas of the hippocampus. The proportion of neurons expressing Arc in the DG enclosed blade did not differ among experimental groups (F=17.14; p<0.0001; Fig. 5a). In contrast, the proportion of neurons expressing Arc in the CA1 differed statistically between groups (F=17.14; p<0.0001; Fig. 5b), where the proportion of Arc immunoreactive neurons found in WT-IRR mice was significantly lower than that of all other groups (post hoc tests: WT-IRR vs. WT-SH, p<0.001, WT-IRR vs. CCR2$^{-/-}$-SH, p<0.001 and WT-IRR vs. CCR2$^{-/-}$-IRR, p<0.001). The proportion of neurons expressing Arc in the CA3 also differed among groups (F=9.868, p=0.0002; Fig. 5c), where the proportion of Arc-positive cells found in WT-IRR mice was significantly lower from all other groups (post hoc tests: WT-IRR vs. WT-SH, p<0.01, WT-IRR vs. CCR2$^{-/-}$-SH, p<0.001 and WT-IRR vs. CCR2$^{-/-}$-IRR, p<0.001).

Discussion

The chemokine receptor CCR2 is constitutively expressed by cells of the monocyte-macrophage lineage (25–27), neural progenitors (31) and hippocampal neurons (32, 33). Considerable data are available regarding how ionizing irradiation affects inflammatory processes (10, 41), the survival, differentiation and migration patterns of neural progenitors cells (8, 9, 12) and hippocampal neuronal function (10). Additionally there are emerging data on the role of the chemokine receptor CCR2 on inflammation and on the progression of different neurodegenerative conditions associated with cognitive dysfunctions (34, 35). Given this information, we hypothesized that a deficiency in CCR2 would impact molecular and cellular mechanisms involved in irradiation-induced brain injury and prevent irradiation-induced cognitive impairments. In order to test this hypothesis we used an established model of cranial irradiation in CCR2 deficient and WT animals (3, 8, 10, 36). Our results demonstrate

NIH-PA Author Manuscript

NIH-PA Author Manuscript

NIH-PA Author Manuscript

that CCR2 deficiency reduces molecular (inflammation-related genes expression) and cellular (plasticity-related immediate early gene *Arc*) aspects of irradiation-induced brain injury and prevents behavioral changes induced by irradiation. These data offer novel insights into the mechanism of radiation-injury and suggest that the monocyte chemoattractant protein-1 receptor CCR2 is a critical mediator of irradiation-induced hippocampal neuronal dysfunction.

Cells of the monocyte-macrophage lineage are mediators of the CNS damage and recovery in neuroinflammatory and neurodegenerative disorders. Among the panel of genes related to inflammation analyzed in the hippocampus following irradiation, we observed a significant upregulation in the transcript levels of CCR2 receptor and of CCL7, CCL8 and CCL12 chemokines that are all ligands for CCR2. CCR2 is considered to be critical for macrophage trafficking and activation in the brain (28–30). Although resident microglia and recruited peripheral macrophages were not distinguished in the present experiment, mice devoid of CCR2 were shown to exhibit reduced infiltration of peripheral macrophages in disease models (29, 30). Recent evidence indicates that the activation of cells of the monocyte-macrophage lineage is a polarized process leading to a potentially neurotoxic M1 “classical activation” or potentially neuroprotective M2 “alternative activation” (26, 42). The regulation of this functional polarization after brain injury is still not clear. To investigate the induction of molecules that characterize the M1 or M2 profile of activation, QPCR gene expression analyses were pursued to reveal iNOS and CD16, key in M1 activation, and the mannose receptor CD206 and Ym1 as part of the M2 molecular repertoire. Interestingly, while the levels of the pan-macrophage activation marker CD68 and M1 markers iNOS and CD16 were not significantly changed, we found increases in the M2 markers CD206 and Ym1 in both irradiated WT and $CCR2^{-/-}$ animals compared with non-irradiated controls. Therefore, our data suggest that monocytes display a neuroprotective phenotype and are involved in remodeling and repair three months after cranial irradiation. Because similar patterns of M2 activation were observed in WT and $CCR2^{-/-}$ animals, our data support the idea that M2 activation is not mediated through CCR2 signaling in our experimental model. As monocyte activation involves a temporally regulated process, future studies will be needed to investigate activation phenotype markers at earlier and later time-point following irradiation.

Adult-born neurons generated in the subgranular zone migrate through the dentate granule layer, integrate into hippocampal networks (12–14) and contribute to hippocampal functions (15, 16). Data from our laboratory have shown the extreme sensitivity of adult-born neurons to irradiation, and altered neurogenesis has been proposed to play a role in irradiation-induced cognitive impairments (3, 8, 9). The present data show reduced neurogenesis in both WT-IRR and $CCR2^{-/-}$-IRR mice. Interestingly, while the reduction in neurogenesis seen in WT-IRR animals paralleled the cognitive impairments measured in the Morris water maze, the changes seen in the $CCR2^{-/-}$ animals did not. This suggests that the relationship between neurogenesis and cognition is complicated.

It has been previously reported by us and others that the distribution patterns of adult-born granule cells through the granule cell layer of the DG changes under pathophysiological conditions such as inflammation (12, 13, 43). Notably, CCR2 is expressed by neural progenitors and regulates their migration (31, 44). Therefore, to further characterize the impact of irradiation on neurogenesis from a functional prospective, we assessed the distribution pattern of the remaining adult-born neurons throughout the DG granule cell layer. In WT-IRR animals, BrdU-labeled new-born neurons were located a longer average distance from the enclosed blade of the dentate granule cell layer compared to controls. It is possible that such a change in the distribution pattern of BrdU-labeled neurons could reflect a selective loss of new-born neurons in the mid third and outer third of the granule cell layer following irradiation. However, while CCR2 deficiency was sufficient to inhibit the change in the distribution pattern of adult-born neurons it did not prevent their overall loss following irradiation. This and similar

NIH-PA Author Manuscript

NIH-PA Author Manuscript

NIH-PA Author Manuscript

observations made in the context of chronic neuroinflammation (13), experimental trauma brain injury (12) and experimental stroke (43) would suggest that the migration pattern of adult-born neurons may change under pathophysiological conditions. The present study is the first *in vivo* demonstration that CCR2 is involved in the distribution pattern of adult-born neurons under pathophysiological conditions. This finding further strengthens the role of CCR2 in irradiation-induced brain injury and the importance of considering CCR2 as a potential therapeutic target to prevent irradiation-induced CNS damage.

The plasticity-related immediate-early gene *Arc* and its protein product Arc are induced in hippocampal pyramidal and granule neurons following spatial exploration in percentages similar to those recorded electrophysiologically (45). Reduction of *Arc* expression through gene disruption (46) or antisense oligonucleotides (45) has been shown to impair spatial learning and long-term potentiation. In the present study, we used the detection of plasticity-related Arc as a reliable method for monitoring neuronal activation reflecting spatial and contextual information processing in response to behavior (21, 23, 47, 48). Our data show that the percentage of pyramidal neurons expressing Arc in the CA1 and the CA3 were significantly decreased in WT-IRR mice compared to non-irradiated WT. Because *Arc* is necessary for synaptic plasticity and memory formation (45, 46), the Arc changes observed here may explain the cellular alterations responsible for radiation-induced cognitive injury. The results reported here demonstrate that irradiation modifies the plasticity-related Arc expression in WT but not in $CCR2^{-/-}$ animals, therefore demonstrating a disruption of behaviorally-induced neuronal activation following irradiation mediated through CCR2. Furthermore, our data evidence a long-term increase in the gene expression of the CCR2 ligands CCL7, CCL8 and CCL12. Chemokines have been shown to play a role in hippocampal neuronal signaling (49) and CCR2 is constitutively expressed by neurons in the granular cell layer of the DG and the pyramidal cell layer CA1 and CA3 area of the hippocampus (32, 33). Therefore, our data strongly suggest that long-term deregulation in CCR2 signaling underlies brain-irradiation. Targeting CCR2 signaling could therefore be a valuable strategy to maintain optimal synaptic plasticity during hippocampal-dependent tasks. Interestingly, our data also show a long-term increase in the gene expression of CCR1 and future studies will be performed to assess its specific role in irradiation induced brain injury.

Behavior data show that irradiation affected hippocampus-dependent functions displayed by delayed spatial learning and impaired memory in the Morris water maze but did not affect hippocampus-independent functions measured by the short delay version of the novel object recognition test. The ability to navigate in the Morris water maze relies on the hippocampus (38). In contrast, short-delay novel object recognition test is not hippocampus dependent but relies on the perirhinal cortex (37, 50). Our behavioral data clearly demonstrated a selective vulnerability of the hippocampus after irradiation. Importantly, here we demonstrated that the CCR2 deficiency prevents the irradiation-induced cognitive deficits. The present study demonstrates that CCR2 deficiency is able to prevent the hippocampal-dependent cognitive impairments induced by therapeutic cranial irradiation. Together the data on hippocampal-dependent cognitive functions and Arc expression in $CCR2^{-/-}$ animals validate the important role for inflammatory factors, specifically the chemokine CCR2, in irradiation-induced injury.

In conclusion, the present study demonstrates a novel role for CCR2 signaling as a critical mediator of irradiation-induced neuronal dysfunction and cognitive impairment. Therefore, targeting CCR2 signaling could provide an effective approach to reduce or prevent the incidence and severity of irradiation-induced brain injury.

Acknowledgments

Grant support

NIH-PA Author Manuscript

NIH-PA Author Manuscript

NIH-PA Author Manuscript

This work was supported by the NIH R01 CA133216 (SR) R01 NS046051 (JRF)

The authors thank Jinghua Yao for her valuable help in processing brain tissues, Sarah Tarver for helping with the fluorescence imaging.

References

1. Abayomi OK. Pathogenesis of irradiation-induced cognitive dysfunction. Acta Oncol. 1996; 35(6): 659–63. [PubMed: 8938210]
2. Robison LL, Green DM, Hudson M, Meadows AT, Mertens AC, Packer RJ, et al. Long-term outcomes of adult survivors of childhood cancer. Cancer. 2005; 104(11 Suppl):2557–64. [PubMed: 16247780]
3. Rola R, Raber J, Rizk A, Otsuka S, VandenBerg SR, Morhardt DR, et al. Radiation-induced impairment of hippocampal neurogenesis is associated with cognitive deficits in young mice. Exp Neurol. 2004; 188(2):316–30. [PubMed: 15246832]
4. Raber J, Rola R, LeFevour A, Morhardt D, Curley J, Mizumatsu S, et al. Radiation-induced cognitive impairments are associated with changes in indicators of hippocampal neurogenesis. Radiat Res. 2004; 162(1):39–47. [PubMed: 15222778]
5. Zhao W, Payne V, Tommasi E, Diz DI, Hsu FC, Robbins ME. Administration of the peroxisomal proliferator-activated receptor gamma agonist pioglitazone during fractionated brain irradiation prevents radiation-induced cognitive impairment. Int J Radiat Oncol Biol Phys. 2007; 67(1):6–9. [PubMed: 17189061]
6. Yazlovitskaya EM, Edwards E, Thotala D, Fu A, Osusky KL, Whetsell WO Jr, et al. Lithium treatment prevents neurocognitive deficit resulting from cranial irradiation. Cancer Res. 2006; 66(23):11179–86. [PubMed: 17145862]
7. Tofilon PJ, Fike JR. The radioresponse of the central nervous system: a dynamic process. Radiat Res. 2000; 153(4):357–70. [PubMed: 10798963]
8. Mizumatsu S, Monje ML, Morhardt DR, Rola R, Palmer TD, Fike JR. Extreme sensitivity of adult neurogenesis to low doses of X-irradiation. Cancer Res. 2003; 63(14):4021–7. [PubMed: 12874001]
9. Monje ML, Mizumatsu S, Fike JR, Palmer TD. Irradiation induces neural precursor-cell dysfunction. Nat Med. 2002; 8(9):955–62. [PubMed: 12161748]
10. Rosi S, Andres-Mach M, Fishman KM, Levy W, Ferguson RA, Fike JR. Cranial irradiation alters the behaviorally induced immediate-early gene arc (activity-regulated cytoskeleton-associated protein). Cancer Res. 2008; 68(23):9763–70. [PubMed: 19047155]
11. Altman J, Das GD. Autoradiographic and histological evidence of postnatal hippocampal neurogenesis in rats. J Comp Neurol. 1965; 124(3):319–35. [PubMed: 5861717]
12. Rosi S, Belarbi K, Ferguson RA, Fishman K, Obenaus A, Raber J, et al. Trauma-induced alterations in cognition and Arc expression are reduced by previous exposure to 56Fe irradiation. Hippocampus. 2012; 22(3):544–54. [PubMed: 21192069]
13. Belarbi K, Arellano C, Ferguson R, Jopson T, Rosi S. Chronic neuroinflammation impacts the recruitment of adult-born neurons into behaviorally relevant hippocampal networks. Brain Behav Immun. 2012; 26(1):18–23. [PubMed: 21787860]
14. Ramirez-Amaya V, Marrone DF, Gage FH, Worley PF, Barnes CA. Integration of new neurons into functional neural networks. J Neurosci. 2006; 26(47):12237–41. [PubMed: 17122048]
15. Jessberger S, Clark RE, Broadbent NJ, Clemenson GD Jr, Consiglio A, Lie DC, et al. Dentate gyrus-specific knockdown of adult neurogenesis impairs spatial and object recognition memory in adult rats. Learn Mem. 2009; 16(2):147–54. [PubMed: 19181621]
16. Goodman T, Trouche S, Massou I, Verret L, Zerwas M, Roullet P, et al. Young hippocampal neurons are critical for recent and remote spatial memory in adult mice. Neuroscience. 2010; 171(3):769–78. [PubMed: 20883747]
17. Monje ML, Vogel H, Masek M, Ligon KL, Fisher PG, Palmer TD. Impaired human hippocampal neurogenesis after treatment for central nervous system malignancies. Ann Neurol. 2007; 62(5):515–20. [PubMed: 17786983]
18. Monje ML, Toda H, Palmer TD. Inflammatory blockade restores adult hippocampal neurogenesis. Science. 2003; 302(5651):1760–5. [PubMed: 14615545]

NIH-PA Author Manuscript

NIH-PA Author Manuscript

NIH-PA Author Manuscript

19. Ekdahl CT, Claasen JH, Bonde S, Kokaia Z, Lindvall O. Inflammation is detrimental for neurogenesis in adult brain. Proc Natl Acad Sci U S A. 2003; 100(23):13632–7. [PubMed: 14581618]
20. Rosi S, Ramirez-Amaya V, Vazdarjanova A, Worley PF, Barnes CA, Wenk GL. Neuroinflammation alters the hippocampal pattern of behaviorally induced Arc expression. J Neurosci. 2005; 25(3):723–31. [PubMed: 15659610]
21. Rosi S, Ramirez-Amaya V, Vazdarjanova A, Esparza EE, Larkin PB, Fike JR, et al. Accuracy of hippocampal network activity is disrupted by neuroinflammation: rescue by memantine. Brain. 2009; 132(Pt 9):2464–77. [PubMed: 19531533]
22. Rosi S, Vazdarjanova A, Ramirez-Amaya V, Worley PF, Barnes CA, Wenk GL. Memantine protects against LPS-induced neuroinflammation, restores behaviorally-induced gene expression and spatial learning in the rat. Neuroscience. 2006; 142(4):1303–15. [PubMed: 16989956]
23. Belarbi K, Jopson T, Tweedie D, Arellano C, Luo W, Greig NH, et al. TNF-alpha protein synthesis inhibitor restores neuronal function and reverses cognitive deficits induced by chronic neuroinflammation. J Neuroinflammation. 2012; 9:23. [PubMed: 22277195]
24. Moser B, Wolf M, Walz A, Loetscher P. Chemokines: multiple levels of leukocyte migration control. Trends Immunol. 2004; 25(2):75–84. [PubMed: 15102366]
25. Sica A, Saccani A, Borsatti A, Power CA, Wells TN, Luini W, et al. Bacterial lipopolysaccharide rapidly inhibits expression of C-C chemokine receptors in human monocytes. J Exp Med. 1997; 185 (5):969–74. [PubMed: 9120403]
26. Martinez FO, Helming L, Gordon S. Alternative activation of macrophages: an immunologic functional perspective. Annu Rev Immunol. 2009; 27:451–83. [PubMed: 19105661]
27. Boddeke EW, Meigel I, Frentzel S, Gourmala NG, Harrison JK, Buttini M, et al. Cultured rat microglia express functional beta-chemokine receptors. J Neuroimmunol. 1999; 98(2):176–84. [PubMed: 10430051]
28. Babcock AA, Kuziel WA, Rivest S, Owens T. Chemokine expression by glial cells directs leukocytes to sites of axonal injury in the CNS. J Neurosci. 2003; 23(21):7922–30. [PubMed: 12944523]
29. Fife BT, Huffnagle GB, Kuziel WA, Karpus WJ. CC chemokine receptor 2 is critical for induction of experimental autoimmune encephalomyelitis. J Exp Med. 2000; 192(6):899–905. [PubMed: 10993920]
30. Prinz M, Priller J. Tickets to the brain: role of CCR2 and CX3CR1 in myeloid cell entry in the CNS. J Neuroimmunol. 2010; 224(1–2):80–4. [PubMed: 20554025]
31. Tran PB, Banisadr G, Ren D, Chenn A, Miller RJ. Chemokine receptor expression by neural progenitor cells in neurogenic regions of mouse brain. J Comp Neurol. 2007; 500(6):1007–33. [PubMed: 17183554]
32. Banisadr G, Queraud-Lesaux F, Boutterin MC, Pelaprat D, Zalc B, Rostene W, et al. Distribution, cellular localization and functional role of CCR2 chemokine receptors in adult rat brain. J Neurochem. 2002; 81(2):257–69. [PubMed: 12064472]
33. van der Meer P, Ulrich AM, Gonzalez-Scarano F, Lavi E. Immunohistochemical analysis of CCR2, CCR3, CCR5, and CXCR4 in the human brain: potential mechanisms for HIV dementia. Exp Mol Pathol. 2000; 69(3):192–201. [PubMed: 11115360]
34. Naert G, Rivest S. CC chemokine receptor 2 deficiency aggravates cognitive impairments and amyloid pathology in a transgenic mouse model of Alzheimer's disease. J Neurosci. 2011; 31(16):6208–20. [PubMed: 21508244]
35. Semple BD, Kossmann T, Morganti-Kossmann MC. Role of chemokines in CNS health and pathology: a focus on the CCL2/CCR2 and CXCL8/CXCR2 networks. J Cereb Blood Flow Metab. 2010; 30(3):459–73. [PubMed: 19904283]
36. Rosi S, Ferguson R, Fishman K, Allen A, Raber J, Fike JR. The polyamine inhibitor alpha-difluoromethylornithine modulates hippocampus-dependent function after single and combined injuries. PLoS One. 2012; 7(1):e31094. [PubMed: 22299052]
37. Mumby DG, Gaskin S, Glenn MJ, Schramek TE, Lehmann H. Hippocampal damage and exploratory preferences in rats: memory for objects, places, and contexts. Learn Mem. 2002; 9(2):49–57. [PubMed: 11992015]
38. Morris RG, Garrud P, Rawlins JN, O'Keefe J. Place navigation impaired in rats with hippocampal lesions. Nature. 1982; 297(5868):681–3. [PubMed: 7088155]

NIH-PA Author Manuscript

NIH-PA Author Manuscript

NIH-PA Author Manuscript

39. Gordon S, Martinez FO. Alternative activation of macrophages: mechanism and functions. Immunity. 2010; 32(5):593–604. [PubMed: 20510870]
40. Ghassabeh GH, De Baetselier P, Brys L, Noel W, Van Ginderachter JA, Meerschaut S, et al. Identification of a common gene signature for type II cytokine-associated myeloid cells elicited in vivo in different pathologic conditions. Blood. 2006; 108(2):575–83. [PubMed: 16556895]
41. Moravan MJ, Olschowka JA, Williams JP, O'Banion MK. Cranial irradiation leads to acute and persistent neuroinflammation with delayed increases in T-cell infiltration and CD11c expression in C57BL/6 mouse brain. Radiat Res. 2011; 176(4):459–73. [PubMed: 21787181]
42. Mosser DM, Edwards JP. Exploring the full spectrum of macrophage activation. Nat Rev Immunol. 2008; 8(12):958–69. [PubMed: 19029990]
43. Kernie SG, Parent JM. Forebrain neurogenesis after focal Ischemic and traumatic brain injury. Neurobiol Dis. 2010; 37(2):267–74. [PubMed: 19909815]
44. Belmadani A, Tran PB, Ren D, Miller RJ. Chemokines regulate the migration of neural progenitors to sites of neuroinflammation. J Neurosci. 2006; 26(12):3182–91. [PubMed: 16554469]
45. Guzowski JF, Lyford GL, Stevenson GD, Houston FP, McGaugh JL, Worley PF, et al. Inhibition of activity-dependent arc protein expression in the rat hippocampus impairs the maintenance of long-term potentiation and the consolidation of long-term memory. J Neurosci. 2000; 20(11):3993–4001. [PubMed: 10818134]
46. Plath N, Ohana O, Dammermann B, Errington ML, Schmitz D, Gross C, et al. Arc/Arg3. 1 is essential for the consolidation of synaptic plasticity and memories. Neuron. 2006; 52(3):437–44. [PubMed: 17088210]
47. Rosi S. Neuroinflammation and the plasticity-related immediate-early gene Arc. Brain Behav Immun. 2011; 25(Suppl 1):S39–49. [PubMed: 21320587]
48. Guzowski JF, McNaughton BL, Barnes CA, Worley PF. Environment-specific expression of the immediate-early gene Arc in hippocampal neuronal ensembles. Nat Neurosci. 1999; 2(12):1120–4. [PubMed: 10570490]
49. Meucci O, Fatatis A, Simen AA, Bushell TJ, Gray PW, Miller RJ. Chemokines regulate hippocampal neuronal signaling and gp120 neurotoxicity. Proc Natl Acad Sci U S A. 1998; 95(24):14500–5. [PubMed: 9826729]
50. Barker GR, Bird F, Alexander V, Warburton EC. Recognition memory for objects, place, and temporal order: a disconnection analysis of the role of the medial prefrontal cortex and perirhinal cortex. J Neurosci. 2007; 27(11):2948–57. [PubMed: 17360918]

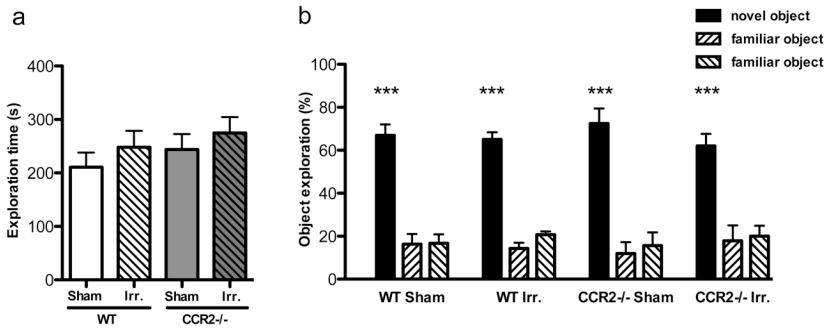

Figure 1. Novel object recognition test

A. Analysis of the total amount of object exploration during the familiarization phase showed no significant difference across experimental groups. **B.** During the test phase, WT-SH, WT-IRR, CCR2$^{-/-}$-SH and CCR2$^{-/-}$-IRR mice all showed a preference for the novel object over the familiar ones (***$p<0.001$ vs. familiar objects).

NIH-PA Author Manuscript NIH-PA Author Manuscript NIH-PA Author Manuscript

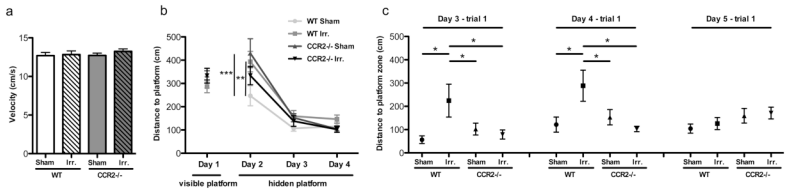

Figure 2. Morris water maze test

A. There was no significant group difference in average swim velocity. **B.** During the visible platform training (day 1), all experimental groups displayed similar distance to the platform. During the hidden platform training (day 2–4), all groups showed daily improvements in their abilities to locate the hidden platform. However, both WT-IRR and $CCR2^{-/-}$-SH mice showed longer escape distance than WT-SH mice on day 2 (**p<0.01; ***p<0.001 vs. WT-SH). **C.** WT-IRR group show higher distance to the platform zone to reach the platform zone on the first trial of day 3 and 4 compared with the other groups (*p<0.05 vs. other groups).

NIH-PA Author Manuscript
NIH-PA Author Manuscript
NIH-PA Author Manuscript

NIH-PA Author Manuscript

NIH-PA Author Manuscript

NIH-PA Author Manuscript

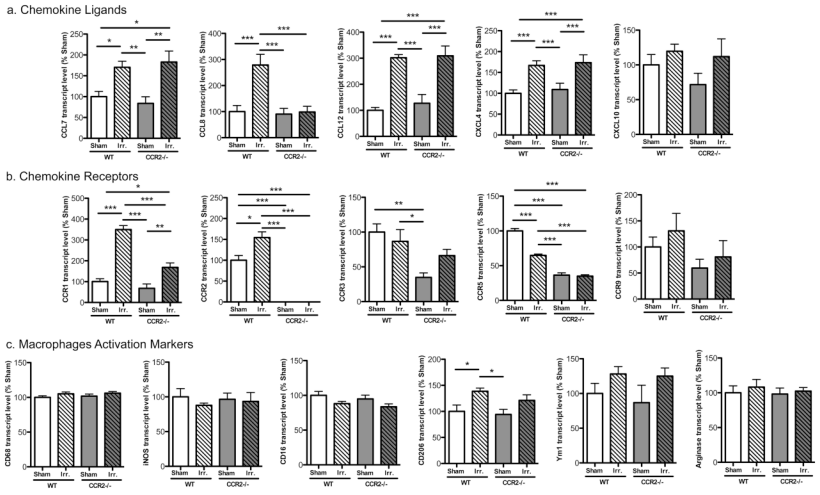

Figure 3. Quantitative RT-PCR analysis of hippocampal samples

A. Gene expression of the chemokine ligands showed that irradiation induced a statistically significant increase in CCL7, CCL8, CCL12 and CXCL4. CCR2 deficiency lowered CCL8 induction. **B.** Gene expression of the chemokine receptors showed that irradiation induced CCR1 and CCR2. CCR2 deficiency lowered CCR1 induction. **C.** Gene expression of the macrophage activation markers iNOS and CD16 (M1 phenotype) showed no significant changes between groups. Similar trends were observed in the M2 phenotype markers CD206 and Ym1 with an increase in gene expression in irradiated WT and CCR2$^{-/-}$ mice. (*p<0.05; **p<0.01; ***p<0.001).

NIH-PA Author Manuscript
NIH-PA Author Manuscript
NIH-PA Author Manuscript

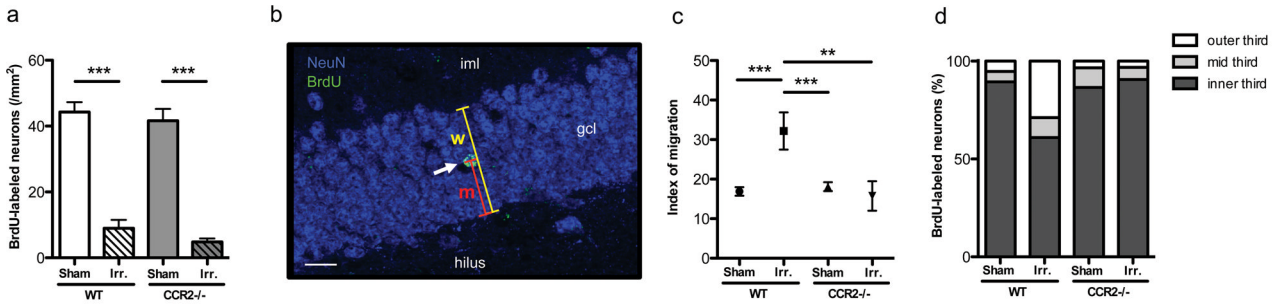

Figure 4. Basal neurogenesis and migration of adult-born neurons

A. The number of BrdU-labeled neurons in the DG enclosed blade was significantly lower in irradiated animals than in non-irradiated ones, independently of the genotype (***p<0.001). **B.** Index of migration was calculated as im = m/w × 100; "m" is the distance between the center of the nucleus and the subgranular zone; "w" is the width of the granule cell layer. **C.** The average index of migration of BrdU-labeled neurons was higher in WT-IRR mice than in WT-SH, $CCR2^{-/-}$-SH and $CCR2^{-/-}$-IRR mice (**p<0.01; ***p<0.001). **D.** Proportions of newly born neurons within the inner, intermediate, and outer third of the DG enclosed blade granule cell layer, for each experimental group.

NIH-PA Author Manuscript

NIH-PA Author Manuscript

NIH-PA Author Manuscript

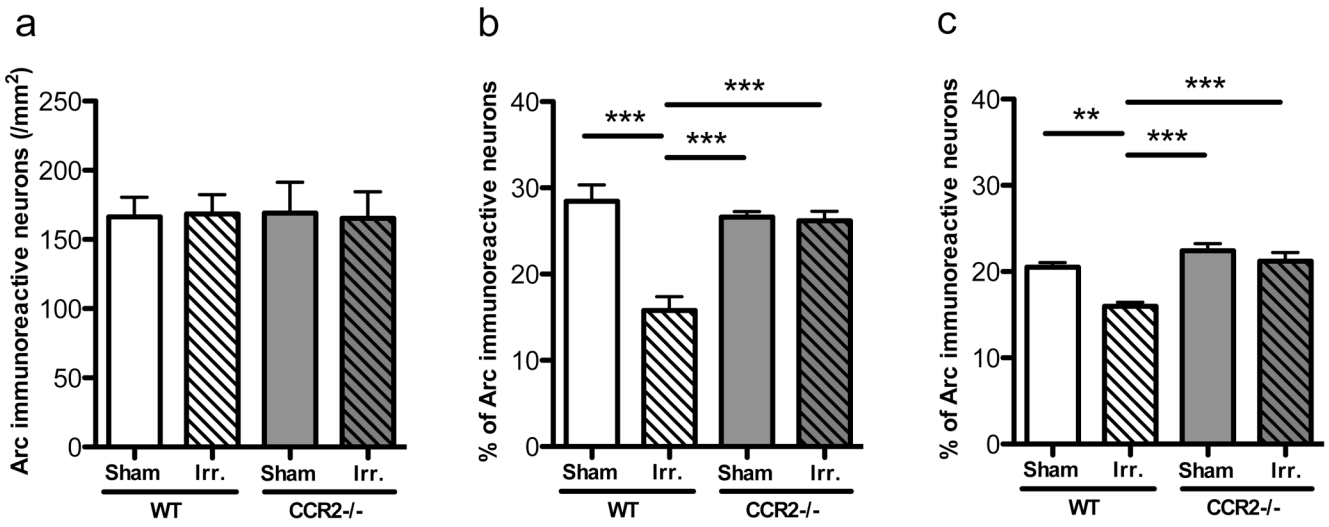

Figure 5. Proportion of neurons expressing Arc in response to behavior

A. The proportion of neurons expressing Arc in the DG enclosed blade did not differ among experimental groups. **B, C.** The proportion of neurons expressing Arc in the CA1 and the CA3 differed statistically between groups, where the proportion of Arc immunoreactive neurons found in WT-IRR mice was significantly higher than that of all other groups (**p<0.01; ***p<0.001).

NIH-PA Author Manuscript

NIH-PA Author Manuscript

NIH-PA Author Manuscript

Table 1

Primer sequences for real-time RT-PCR analysis

Gene	GenBank accession number	Forward primer 5′→3′	Reverse primer 5′→3′
Arginase	NM_007482	GAACACGGCAGTGGCTTTAAC	TGCTTAGCTCTGTCTGCTTTGC
CCL7	NM_013654	TGGGAAGCTGTTATCTTCAAGACA	CTCGACCCACTTCTGATGGG
CCL8	NM_021443	GCAGTGCTTCTTTGCCTGCT	ACAGCTTCCATGGGGCACT
CCL12	NM_011331	CAGTCCTCAGGTATTGGCTGGA	TCCTTGGGGTCAGCACAGAT
CCR1	NM_009912.4	TTCCTCCTCTGGACCCCCTA	TTGAAACAGCTGCCGAAGGT
CCR2	NM_009915.2	CCACACCCTGTTTCGCTGTA	TGCATGGCCTGGTCTAAGTG
CCR3	NM_009914	CCACTGTACTCCCTGGTGTTCA	GGACAGTGAAGAGAAAGAGCAGG
CCR5	NM_009917	CAGGGCTGTGAGGCTCATCT	GGCAGCAGTGTGTCATTCCA
CCR9	NM_009913	GGTCACCTTGGGGTTTTTCC	TAAGCGTCAACAGCCTGCAC
CD16	NM_010188	TGTTTGCTTTTGCAGACAGG	CGTGTAGCTGGATTGGACCT
CD68	NM_010927	GACCTACATCAGAGCCCG	CGCCATGAATGTCCACTG
CD206	NM_008625	CCTCTGGTGAACGGAATGAT	CTTCCTTTGGTCAGCTTTGG
CXCL4	NM_019932	CCGAAGAAAGCGATGGAGATCT	CCAGGCAAATTTTCCTCCCA
CXCL10	NM_021274	CCTCATCCTGCTGGGTCTG	CTCAACACGTGGGCAGGA
iNOS	NM_010927	GTTCTCAGCCCAACAATACAAGA	GTGGACGGGTCGATGTCAC
Ym1	M94584	GGCTACACTGGAGAAAATAGTCCCC	CCAACCCACTCATTACCCTGATAG

NIH-PA Author Manuscript
NIH-PA Author Manuscript
NIH-PA Author Manuscript

Cancer Res. Author manuscript; available in PMC 2014 February 01.

Table 2

PCR-based array gene expression analyses

			WT irradiated vs. WT sham		CCR2−/− sham vs. WT sham		CCR2−/− irradiated vs. CCR2−/− sham		CCR2−/− irradiated vs. WT−/− irradiated	
Symbol	**Accession**	**Description**	**Fold change**	***p* value**	**Fold change**	***p* value**	**Fold change**	***p* value**	**Fold change**	***p* value**
Chemokine ligands										
Ccl7	NM_013654	Chemokine (C-C motif) ligand 7	2.8945	0.0087	1.3232	0.5295	2.4138	0.0380	1.1034	0.5580
Ccl8	NM_021443	Chemokine (C-C motif) ligand 8	11.1065	0.0079	−1.2053	0.7210	2.9649	0.0775	−4.5148	0.0150
Ccl12	NM_011331	Chemokine (C-C motif) ligand 12	3.0667	0.0063	1.0074	0.9823	3.7965	0.0119	1.2472	0.1614
Cxcl4	NM_019932	Chemokine (C-X-C motif) ligand 4	1.4439	0.0063	1.2900	0.2553	1.6911	0.0411	1.5108	0.0121
Cxcl10	NM_021274	Chemokine (C-X-C motif) ligand 10	1.1147	0.5499	−1.4804	0.0322	1.9743	0.0469	1.1964	0.4850
Chemokine receptors										
Ccr1	NM_009912	Chemokine (C-C motif) receptor 1	9.2108	0.0004	−1.4942	0.2558	4.5357	0.0044	−3.0342	0.0017
Ccr3	NM_009914	Chemokine (C-C motif) receptor 3	−1.6974	0.0639	−5.4743	0.0299	2.4646	0.4237	−1.3086	0.1865
Ccr5	NM_009917	Chemokine (C-C motif) receptor 5	−1.3287	0.0638	−3.7912	0.0005	1.3768	0.2782	−2.0724	0.0127
Ccr9	NM_009913	Chemokine (C-C motif) receptor 9	−1.2864	0.6672	−3.7390	0.0028	1.7387	0.0191	−1.6717	0.2498
Interleukin receptors										
Il2rg	NM_013563	Interleukin 2 receptor, gamma chain	1.4340	0.2860	−1.3342	0.3395	1.8851	0.0077	−1.0149	0.7647
Others										
Spp1	NM_009263	Secreted phosphoprotein 1	1.2864	0.2058	−1.0862	0.6766	1.6911	0.0337	1.2103	0.3391

Regulated genes with fold changes ≥1.5, either up (in red) or down (in blue) and p values ≤ 0.05 for at least one experimental group are presented.